materials proceedings

MDPI

Proceeding Paper

Increasing Resource Efficiency of Bauxites Using LIBS †

Jeannet A. Meima [1,*], Beate Orberger [2,3,*], Carlos García Piña [4], Antoine Prudhomme [2,5] and Carsten Dittrich [6]

1 Bundesanstalt für Geowissenschaften und Rohstoffe (BGR), Stilleweg 2, 30655 Hannover, Germany
2 GEOPS Université Paris Saclay, Bât 504, 92405 Orsay, France; antoine.prudhomme@eramet.com
3 CATURA Geoprojects-Géosciences Conseil, 2 rue Marie Davy, 75014 Paris, France
4 DMT GmbH & Co. KG, Am Tüv 1, 45307 Essen, Germany; carlos.garciapina@dmt-group.com
5 ERAMET, 1 Avenue Albert Einstein, 78190 Trappes, France
6 MEAB Chemie Technik GmbH, Dennewartstraße 25, 52068 Aachen, Germany; carsten@meab-mx.com
* Correspondence: jeannet.meima@bgr.de (J.A.M.); beate.orberger@catura.eu (B.O.)
† Presented at International Conference on Raw Materials and Circular Economy, Athens, Greece, 5–9 September 2021.

Abstract: The EU aluminium production from, e.g., bauxite is one of the backbones to support Europe's green and digital transition. In support of sustainable bauxite exploration and mining, Laser Induced Breakdown Spectroscopy (LIBS) was used on the major facies of the karst bauxite deposits of SODICAPEI (Southern France). Our results showed that LIBS is a very promising technology to define the bottom and top layer of bauxite ores and to access critical parameters crucial for bauxite mining and processing. First LIBS tests were made on scandium standards to find appropriate Sc emission lines for future applications.

Keywords: bauxite; Laser Induced Breakdown Spectroscopy (LIBS); scandium; titanium; aluminium; exploration; processing

Citation: Meima, J.A.; Orberger, B.; García Piña, C.; Prudhomme, A.; Dittrich, C. Increasing Resource Efficiency of Bauxites Using LIBS. *Mater. Proc.* **2021**, *5*, 81. https://doi.org/10.3390/materproc2021005081

Academic Editor: Anthimos Xenidis

Published: 14 December 2021

1. Introduction

Bauxite is formed through weathering of aluminium (Al) rich rocks which are low in alkalis, alkaline earths, and silica [1]. Bauxite is, at present, the only primary aluminium resource: 85% of the mined bauxite is refined into alumina, an intermediate product (Bayer process), which is then smelted (Hall–Heroult process) into aluminium. A total of 10% of the bauxite goes to non-metal products and 5% to refractory and abrasive materials [2] (in [3]). Producing 1 ton of aluminium needs 4–6 t of bauxite (depending on the grade and quality). Alumina is also used in chemical grade applications [4]. The EU Al production is crucial to support the Europe's green and digital transition. It is one of the major metals used in the transportation-automotive, truck, building and constructions, and packaging sectors [4].

Global demand for primary Al from bauxite alone is expected to increase 4% per year until 2030. Today, Europe only produces around 10% of the bauxite for its primary Al, with an increasing import rate [5]. Major producers are Australia, China, Brazil, Guinea, and India [4], while major reserves are available in Guinea (7.4 bt), Australia (6 bt), Brazil (2.6 bt), Vietnam (3.7 bt), Jamaica (2 bt), and Indonesia (1 bt) [6].

Most bauxites (88%) belong to the laterite type concentrated around the equator in the southern hemisphere. It occurs as extended layers over hundreds of square kilometres of highly variable thicknesses (<1 m to 40 m). Minor deposits (12%) are of karst type and karst-related type bauxite concentrated on the northern hemisphere [3,7,8].

In Europe, Karst-type deposits occur in Greece, Hungary, Serbia and Romania, and southern France. Karst bauxites are more difficult to evaluate for resources and reserves. The Karst pockets have variable morphologies, and tens to more than hundred meters of overburden. Bauxite is mainly mined in large open pits and only rarely as underground operations, presenting a high environmental impact and high risk for the ecological system

(water, soils, air, and biodiversity). The goal of the Al industries is sustainable bauxite mining and processing, reducing environmental impacts, and increasing social acceptance.

Bauxite is composed of the Al hydroxides boehmite [γ -AlO(OH)], diaspore [α-AlO(OH)] and gibbsite [$Al(OH)_3$], various iron oxyhydroxides (e.g., goethite [FeO(OH)] and hematite [Fe_2O_3]), anatase/rutile [TiO_2], pyrite [FeS_2], clay minerals (kaolinite[$Al_2Si_2O_5(OH)_4$] and montmorillonite [$(Na,Ca)_{0.3}(Al,Mg)_2Si_4O_{10}(OH)_2 \cdot n{\cdot}H_2O$]), quartz [$SiO_2$], carbonates (e.g., siderite [$FeCO_3$]), phosphate minerals, corundum [Al_2O_3], and zircon [$ZrSiO_4$]. Amorphous and poorly crystalline phases are also present [9]. The underlying carbonates are mainly calcite or dolomite. Overburden consists of sandstones, silt, and claystones hosting various amounts of carbonates and iron oxyhydroxides, e.g., [9].

Challenges in bauxite deposits relate to the mineralogy and chemistry to ecologically and economically recover Al_2O_3, the abundance of Al-bearing minerals and contaminant minerals/elements. (1) The presence of reactive SiO_2 in aluminosilicates as well as TiO_2 negatively influence the Bayer process, increasing energy and flocculent consumption. (2) The bauxite/Al_2O_3-ratio and bauxite /reactive Al_2O_3 ratio indicate how much bauxite needs to be extracted to produce 1 t of alumina. (3) The moisture content refers to water that is not bound in mineral structures, which at high amounts, however, increases transport and processing costs. (4) The waste/ore ratio is crucial for environmental mine and processing planning. (5) The land use/t reactive Al_2O_3 gives information on the surface impacted by open pit mining per ton of bauxite. These data depend on geometry, volume, and grade of the orebody [3]. It is thus crucial that exploration and mining companies have the most exact 3D geological models for accessing the above-mentioned parameters in order to optimize mining and processing, to increase the resource efficiency. Furthermore, bauxite residues after Al production provide resources for scandium (Sc), a rare element and critical element for the EU as it has a growing market in AlSc master alloy industries and the EU is 100% depend on imports (https://scaletechnology.eu/) (accessed on 3 December 2021).

LIBS is a promising multi-elemental technology for application in core scanners and industrial instrumentation to investigate compositional variations in rocks and sediments, e.g., [10,11]. The technology is based on atomic emission spectroscopy, in which the excitation of the atomic species occurs in situ on the sample surface using a highly energetic pulsed laser, e.g., [12,13]. Of particular interest is its ability to measure light elements [14] as well as its speed of measurement [11]. The development of calibration and classification methods for LIBS applications is an ongoing area of research, as plasma variations can severely affect the LIBS spectra, e.g., [13–16]. Plasma variations may be sample-unspecific or relate to chemical or physical variations on the sample surface, which is why LIBS analysis is very challenging for geological applications in laboratory, field, or industrial surroundings. Calibrated LIBS data can be considered as semi-quantitative as compared to conventional laboratory analyses. Excellent reviews are presented by, e.g., [13,14]. Scandium applications are difficult to find in the LIBS literature, but emission lines for Sc are documented in [17,18].

In this paper, LIBS was used to characterize the different bauxite facies, to localize the shale marker horizon, the onset of bauxite, the base of bauxite, and the contact to the karst pocket. First tests were made on scandium standards to find appropriate scandium emission lines for future applications.

2. Materials and Methods

The samples analysed here represent the major facies of the karst bauxite deposits (SODICAPEI), located north of Villeveyrac, Southern France. The top layer facies, the bauxite, and the underlying carbonate karst dolomitized limestone were sampled from drill core FT 184. The samples cover the profile from bottom to top (Figure 1, right to left): bottom dolomitized limestone (karst) (ER-SD00-0100), pisolitic bauxite (ER-SD00-0101), red bauxite (ER-SD00-0102), pisolitic bauxite (ER-SD00-0103), pisolitic bauxite conglomerate (ER-SD00-0104), red-clay with bauxite ER-SD00-0105), the marker horizon, black shale (ER-SD00-0106), marl (ER-SD00-0107), and sandy shale (ER-SD00-0108). The black shale

represents a marker horizon, defining the proximity of the onset of the bauxite. This layer is oxidized in some part, being present as red shale in some parts of the mine site.

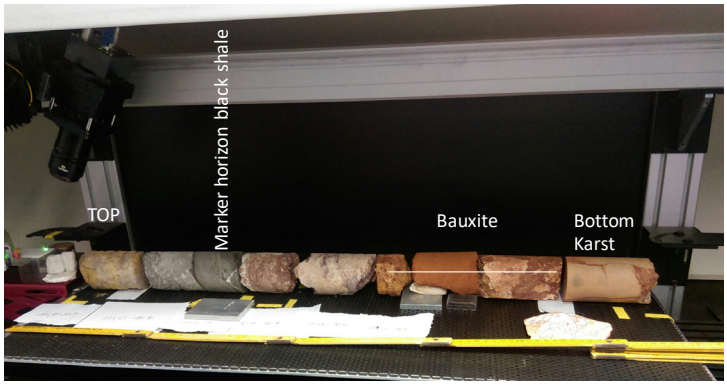

Figure 1. LIBS measurement configuration of composite bauxite profile.

All samples were studied by laboratory XRF and XRD (ERAMET IDEAS) and portable infrared (BRGM) in the frame of the SOLSA project [19]. Sandy shales are composed of calcite, kaolinite, illite, vermiculite and/or smectite, goethite, quartz, and gypsum ($CaSO_4$ 2 H_2O). The marls have the same mineralogical composition, but do not show goethite. Carbonated black shales, here the marker horizon, are similar in composition as sandy shale and marls, have no vermiculite smectite, no goethite, but pyrite. The onset of bauxite is indicated by marls and pisolitic bauxite with similar composition as the previous lithologies, and with the appearance of anatase (TiO_2). Bauxite layers are rich in boehmite, hematite, rutile, and anatase, and may host zircon. The bottom layer carbonate is mainly composed of calcite, hematite, goethite, and kaolinite.

LIBS measurements were performed with the prototype core scanner from LTB (2011), using a Nd:YAG 1064 nm laser (35 mJ, 5.5 ns, 20 Hz) and an Echelle spectrometer covering 285 nm–960 nm at a resolution of 28–94 pm [10]. The laser spot size was about 200 µm. Dust particles were kept away from the spot area by air suction. Figure 1 visualizes the core arrangement, on which 4275 LIBS measurements were collected with a distance of 200 µm between shots. Each single LIBS measurement consisted of one cleaning shot and 3 accumulated measuring shots. Data processing relies on the intensity of several characteristic emission lines for Al, Si, K, Ca, C, S, Ti, and Fe, as well as on the total spectral intensity for normalization purposes. Measurements that were out of focus were removed from the dataset. A calibration of the LIBS data was not attempted, as it was the objective of this study to investigate whether similarities and/or differences between samples can be recognized in the raw LIBS data.

First tests on Sc detection with LIBS were performed on Sc_2O_3 concentrate produced during the H2020 SCALE project, and also on the NIST-610 standard containing 500 ppm Sc. The Sc_2O_3 powder was pressed to a pellet without using additives. The LIBS spectrum of the Sc_2O_3 concentrate was measured with 1 cleaning shot and 1 measuring shot, and the LIBS spectrum of the NIST-610 standard with 5 accumulated measuring shots.

3. Results and Discussion

Figure 2 shows exemplary LIBS spectra from the four key horizons: black shale, marl, red bauxite, and bottom limestone. The black shale horizon is dominated by Fe emission lines, but also shows significant emission of, e.g., Al, Ca, and S. Emission lines for C were detected in some of the neighbouring spectra, possibly representing organic material. The marl horizon is dominated by Ca emission lines, but also shows emission lines for, e.g., Al, Fe, and Ti. The red bauxite horizon is dominated by Al, Ti, and Fe emission lines. The bottom carbonate horizon is dominated by Ca-emission lines, as well as an increased emission of molecular species in the region between 550 and 650 nm.

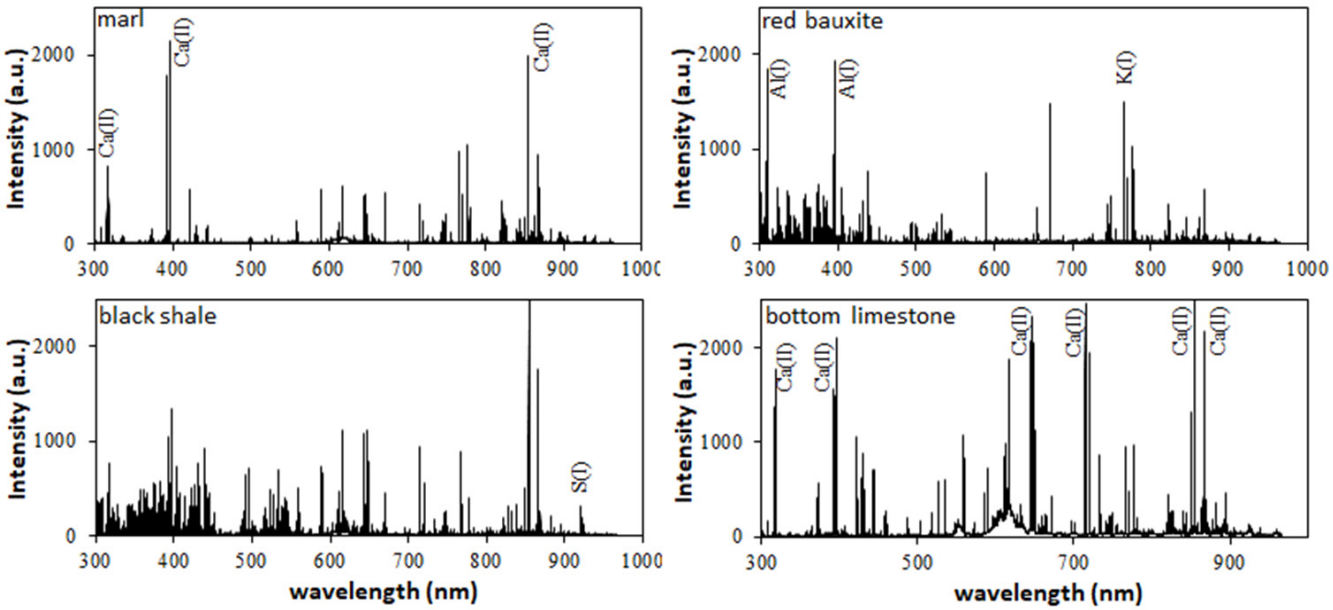

Figure 2. Exemplary LIBS spectra for marl, black shale, red bauxite, and limestone.

Figure 3 shows the composite bauxite profile with the observed LIBS intensities for selected emission lines. The different facies could be well distinguished with LIBS. The black shale horizon can easily be characterized by the increased S emission. The bauxite onset is recognised by the sudden decrease in Ca and increase in Al emission. The bauxite/karst boundary is recognised by a sudden increase in Ca and decrease in Al emission. The brecciated bauxite shows already Ca. Other target elements (e.g., Si, Fe, Ti, Mg, Na, K, and Li) support these observations and/or provide additional data. Classification of the LIBS data was found to be very effective to identify key horizons (results not shown).

Figure 3 also shows Ti enrichments in the brecciated bauxite, possibly representing rutile/anatase. Anatase is a heavy mineral, and it may be due to gravity that it is enriched in the brecciated part. The mineral is harmful for machines used in ore preparation due to its abrasive character. Titanium is generally easily detected with LIBS due to its many moderate and strong emission lines (e.g., [17,18]). Another highly abrasive target mineral is quartz, which can also be detected with LIBS. In case of very fine-grained material such as bauxite, SiO_2 contents can be obtained from calibrated LIBS data.

Scandium has a very large number of potential emission lines, and many of them were detected in the Sc_2O_3 concentrate with our LIBS system. On the NIST610 standard that contains 500 ppm Sc, we could measure weak Sc emission around 360 nm (Figure 4), which is in line with the Sc spectrum in [18].

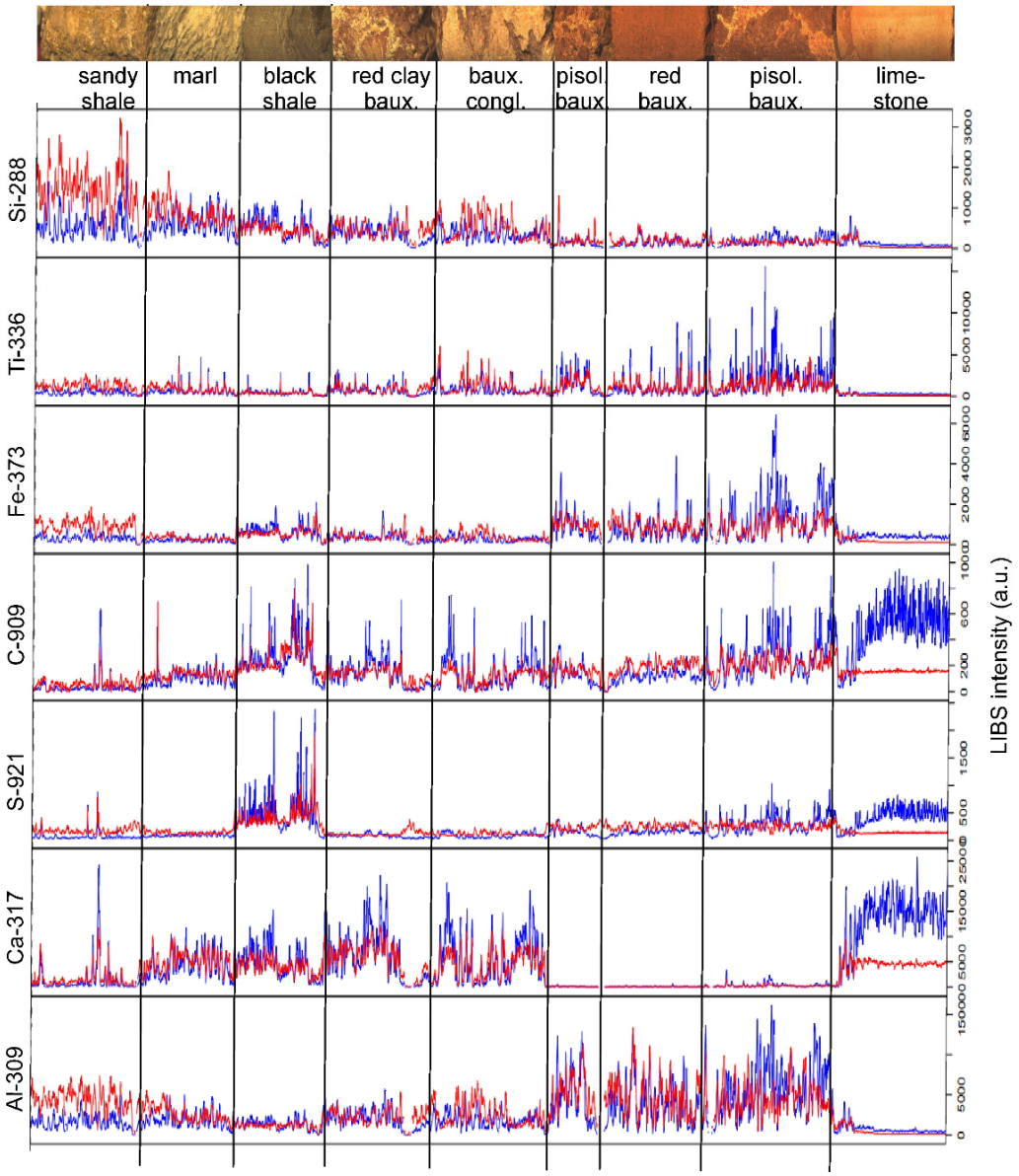

Figure 3. Uncalibrated LIBS intensities for the composite bauxite profile shown at the top. Red lines represent normalized data, blue lines not-normalized data. A running average filter of 5 was applied to reduce noise and small-scale variations in the data. Unfiltered data are shown for S-921, C-909, and Ti-336, above intensity-thresholds of 500, 500, and 2500, respectively.

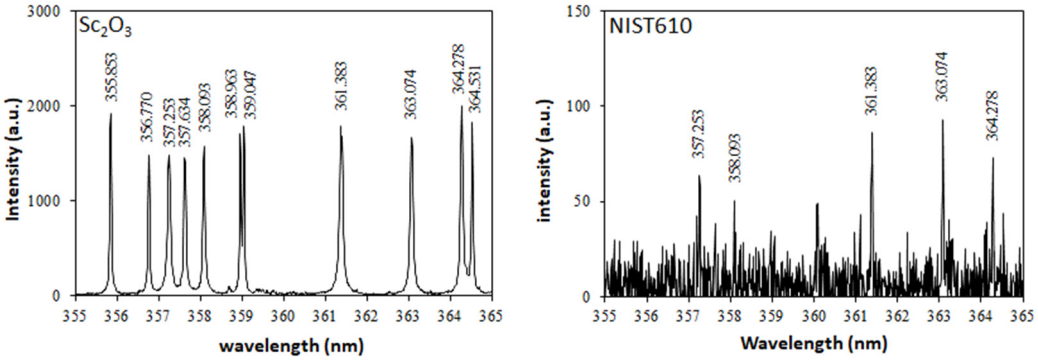

Figure 4. LIBS spectral region 355–365 nm with Sc II lines for the Sc_2O_3 concentrate and NIST610 standard.

4. General Discussion

Sustainable bauxite exploration and mining could benefit from LIBS for several reasons: (1) Rapid identification and analysis of the bauxite layer and contaminating elements or minerals (e.g., quartz, anatase); (2) Semi-quantitative chemical analyses on drill cores or in open pits in only a few seconds and without the need for sample preparation; this could be realized with appropriate reference samples and a multivariate calibration model (e.g., [10]); (3) Reducing laboratory analyses to the most relevant samples, saving costs and time; (4) Fast decision making during exploration, due to immediate availability of the data; (5) LIBS helps leaving the maximum waste behind during mining and producing minimum waste during processing. In the same way, LIBS can be used along the value chain of processing and waste recycling. Metallurgical waste, the bauxite residue after aluminium production, hosts valuable elements, such as Sc, Ga, and REE, which are going to be extracted in the future at an industrial scale in the EU.

Author Contributions: Conceptualization, investigation, validation, and writing—original draft preparation: J.A.M. (LIBS) and B.O. (review on bauxite deposits; coordination of bauxite petrologic characterization); Methodology, formal analysis, and visualization: J.A.M. (LIBS); Investigation: A.P. (Bauxite characterization); Resources: C.D. (Sc_2O_3 concentrate); Project administration, funding acquisition: C.G.P. (ANCORELOG); Writing—review and editing: all Authors. All authors have read and agreed to the published version of the manuscript.

Funding: This research was funded by EIT RawMaterials (ANCORELOG, No. 17028) and Horizon2020 (SOLSA, No. 689868).

Acknowledgments: We thank the EIT RawMaterials ANCORELOG project (No. 17028) and the H2020 SOLSA project (No. 689868) for financial support.

Conflicts of Interest: The authors declare no conflict of interest. The funders had no role in the design of the study; in the collection, analyses, or interpretation of data; in the writing of the manuscript, or in the decision to publish the results.

References

1. Gow, N.N.; Lozej, G.P. Bauxite. In *Ore Depost Models, Volume II*; Sheaham, P.A., Cherry, M.E., Eds.; Geol. Association Canada: St. John's, NL, Canada, 1993; Volume 20, p. 154.
2. Plunkert, P.A. Bauxite and Alumina. In *Minerals Yearbook 2001: Volume I.—Metals and Minerals*; U.S. Geol. Survey: Reston, VA, USA, 2001.
3. Meyer, F.M. Availability of Bauxite Reserves. *Nat. Resour. Res.* **2004**, *13*, 161–172. [CrossRef]
4. World Aluminium Sustainable Bauxite Mining Guideline (1st Edition). 2018. Available online: www.world-aluminium.org (accessed on 16 June 2021).
5. Bloxome, N. Bauxite Recognised as "Critical Raw Material". Available online: https://aluminiumtoday.com/news/bauxite-recognised-as-critical-raw-material (accessed on 16 June 2021).
6. USGS Global Bauxite Reserves, Bauxite and Alumina Mineral Commodity Summaries. Available online: https://minerals.usgs.gov/minerals/pubs/commodity/bauxite/ (accessed on 16 June 2021).
7. Bárdossy, G. Karst Bauxites: Bauxite Deposits on Carbonate Rocks. In *Developments in Economic Geology*; Elsevier Scientific Pub. Co.: New York, NY, USA; Distribution for the U.S.A. and Canada, Elsevier/North Holland: Amsterdam, The Netherlands, 1982; ISBN 978-0-444-99727-2.
8. Bárdossy, G.; Aleva, G.J.J. Lateritic Bauxites. In *Developments in Economic Geology*; Elsevier Scientific Pub. Co.: New York, NY, USA; Distribution for the U.S.A. and Canada, Elsevier/North Holland: Amsterdam, The Netherlands, 1990; ISBN 978-0-444-98811-9.
9. Sidibe, M.; Yalcin, M.G. Petrography, Mineralogy, Geochemistry and Genesis of the Balaya Bauxite Deposits in Kindia Region, Maritime Guinea, West Africa. *J. Afr. Earth Sci.* **2019**, *149*, 348–366. [CrossRef]
10. Kuhn, K.; Meima, J.A.; Rammlmair, D.; Ohlendorf, C. Chemical Mapping of Mine Waste Drill Cores with Laser-Induced Breakdown Spectroscopy (LIBS) and Energy Dispersive X-Ray Fluorescence (EDXRF) for Mineral Resource Exploration. *J. Geochem. Explor.* **2016**, *161*, 72–84. [CrossRef]
11. Rifai, K.; Michaud Paradis, M.-C.; Swierczek, Z.; Doucet, F.; Özcan, L.; Fayad, A.; Li, J.; Vidal, F. Emergences of New Technology for Ultrafast Automated Mineral Phase Identification and Quantitative Analysis Using the CORIOSITY Laser-Induced Breakdown Spectroscopy (LIBS) System. *Minerals* **2020**, *10*, 918. [CrossRef]
12. Cremers, D.A.; Radziemski, L.J. *Handbook of Laser-Induced Breakdown Spectroscopy*, 1st ed.; Wiley: Chichester, UK; Hoboken, NJ, USA, 2006; ISBN 978-0-470-09299-6.

13. Hahn, D.W.; Omenetto, N. Laser-Induced Breakdown Spectroscopy (LIBS), Part II: Review of Instrumental and Methodological Approaches to Material Analysis and Applications to Different Fields. *Appl. Spectrosc.* **2012**, *66*, 347–419. [CrossRef] [PubMed]
14. Harmon, R.S.; Senesi, G.S. Laser-Induced Breakdown Spectroscopy—A Geochemical Tool for the 21st Century. *Appl. Geochem.* **2021**, *128*, 104929. [CrossRef]
15. Galbács, G. A Critical Review of Recent Progress in Analytical Laser-Induced Breakdown Spectroscopy. *Anal. Bioanal. Chem.* **2015**, *407*, 7537–7562. [CrossRef]
16. Clegg, S.M.; Wiens, R.C.; Anderson, R.; Forni, O.; Frydenvang, J.; Lasue, J.; Cousin, A.; Payré, V.; Boucher, T.; Dyar, M.D.; et al. Recalibration of the Mars Science Laboratory ChemCam Instrument with an Expanded Geochemical Database. *Spectrochim. Acta Part B At. Spectrosc.* **2017**, *129*, 64–85. [CrossRef]
17. Kramida, A.; Ralchenko, Y.; Reader, J. NIST ASD Team NIST Atomic Spectra Database (Version 5.3). Available online: https://physics.nist.gov/asd (accessed on 26 October 2015).
18. Kramida, A.; Olsen, K.; Yu, R. NIST LIBS Database. Available online: https://physics.nist.gov/PhysRefData/ASD/LIBS/libs-form.html (accessed on 16 June 2021).
19. Prudhomme, A. Characterization of a Bauxite Core Using Several Field and Laboratory Methods. Master's Thesis, Université Paris Saclay-ERAMET, France, 2018; p. 20.